Int. J. Environ. Res., 8(3):687-710,Summer 2014
ISSN: 1735-6865

Peat Water Treatment using Chitosan-Silica Composite as an Adsorbent

Zulfikar, M. A.[1*], Setiyanto, H.[1] Wahyuningrum,D.[2] and Mukti,R. R.[3]

[1]Analytical Chemistry Research Group, Institut Teknologi Bandung, Jl. Ganesha 10 Bandung, Indonesia

[2]Organic Chemistry Research Group, Institut Teknologi Bandung, Jl. Ganesha 10 Bandung, Indonesia

[3]Physical and Inorganic Chemistry Research Group, Institut Teknologi Bandung, Jl. Ganesha 10 Bandung, Indonesia

Received 8 Aug. 2013; Revised 4 Nov. 2013; Accepted 9 Nov. 2013

ABSTRACT: The objective of this study is synthesis and characterization of the chitosan-silica composite (CSC) and use them as an adsorbent material for peat water treatment. The resulting composite was characterized by Fourier transform infrared (FTIR) spectroscopy, scanning electron microscope (SEM), X-ray diffraction (XRD), N_2 adsorption-desorption isotherm and zeta potential. The sorption experiments were carried out in batch mode to optimize various parameters such as contact time, dose of CSC, pH and temperature. In addition, adsorption isotherms of humic acid onto the CSC were also evaluated with the Langmuir, Freundlich and Sips approximations. Kinetic data were tested using the pseudo-first-order, pseudo-second-order kinetic models and intra-particle equations. The results from this work showed that the adsorption of humic acid was found to increase with increase in contact time and temperature while acidic pH was more favorable for the adsorption of humic acid from peat water. The optimum dosage of CSC was 5 g. Equilibrium data were best described by the Langmuir isotherm model, with maximum monolayer adsorption capacity of 120.2 mg/g at 25 ^oC and pH 4.12. The kinetics of the adsorption process was found to follow the pseudo-second-order kinetic model, with a rate constant in the range of 0.034 - 0.105 g/mg/min, while intra-particle-diffusion were the main rate determining step in the humic acid adsorption process. Thermodynamic parameters data indicated that the humic acid sorption process was non-spontaneous and endothermic under the experimental conditions, with the Gibbs free energy ("G^o) in the range of 1.05-3.89 kJ/mol, enthalpy ("H^o) and entropy ("S^o) of 24.69 kJ/mol and 69.62 J/mol, respectively and the activation energy was 23.23 kJ/mol. The CSC investigated in this study thus exhibited as a high potential adsorbent for the peat water treatment.

Key words: Adsorption, Chitosan-silica, Humic acid, Peat water, Removal

INTRODUCTION

Peat water is a heterogeneous mixture of organic compounds which vary in terms of molecular weight (MW), chemical structure and functional groups. Peat water is often fractioned on the basis of hydrophobicity and molecular size (Abate and Masini, 2003; Rojas *et al*., 2011) and therefore includes a set of hydrophilic substances, particularly aliphatic carbon and nitrogenous compounds (sugars, carbohydrates, amino acids etc.) (Abate and Masini, 2003; Albers *et al*., 2008; Rojas *et al*., 2011), and a set of hydrophobic substances, consisting principally of humic compounds (humic and fulvic acids), noted for their aromaticity and carboxylic and phenolic acid functionality.

*Corresponding author E-mail:zulfikar@chem.itb.ac.id

Of these substances, hydrophobic humic acid compounds tend to react with a variety of oxidants and disinfectants to form carcinogenic disinfection byproducts (DBPs) such as trihalomethanes and haloacetic acids during drinking water production. At the same time, humic acid may cause water to have color, taste and odor, and bind heavy metals, making water treatment necessary.

At present, there are several methods used to remove humic acid as main component from peat water, such as coagulation-flocculation (Uygunera *et al*., 2007; Libecki and Dziejowski, 2008; Park *et al*., 2009; Rojas *et al*., 2011; Sun *et al*., 2011;), electro coagulation

processes (Ghernaout *et al*., 2009; Wang *et al*., 2011), oxidation (Uygunera *et al*., 2007; Libecki and Dziejowski, 2008), photocatalysis (Sonea *et al*., 2010) and membrane technology (Park *et al*., 2009; Katsoufidou *et al*., 2010; Hamid *et al*., 2011; Rojas *et al*., 2011). All of these alternative processes, however, are high operational cost and none of them therefore, is considered by industries to be commercially viable because economically unrealistic.

Due to it's easy to operate and most effective, adsorption has been considered as one of the most economically promising techniques for the water and wastewater treatments (Gupta *et al*., 2007). In the past years, several adsorbents have been employed for humic acid adsorption including activated carbon (Garcia *et al*., 1998; Daifullah *et al*., 2004; Maghsoodloo *et al*., 2011), fly ash (Wang and Zhu, 2007; Wang *et al*., 2008; Wang *et al*., 2009), *Shorea dasyphylla* sawdust (Kamari *et al*., 2009), eggshell (Zulfikar *et al*., 2013a), zeolite (Moussavi *et al*., 2011), clay mineral (Peng *et al*., 2005; Salman *et al*., 2008; Doulia *et al*., 2009; Zhang *et al*., 2012), chitosan (Ngah *et al*., 1998; Ngah *et al*., 2011), chitin (Ngah *et al*., 1998), silica (Liang *et al*., 2011) and other adsorbents (Abate and Masini, 2003; Zhang and Bai, 2003; Anirudhan *et al*., 2007; Ngah *et al*., 2008; Zhao *et al*., 2008; Tao *et al*., 2010; Wang *et al*., 2011; Lin and Zhan, 2012).

Chitosan is a nitrogenous polysaccharide composed mainly of poly (β-1-4)-2-amino-2-deoxy-D-glucopyranose and is produced through the deacetylation of chitin (Ngah *et al*., 2008; Maghsoodloo *et al*., 2011; Ngah *et al*., 2011. Chitosan is a natural adsorbent due to the presence of the amine ($-NH_2$) and hydroxyl (-OH) groups and serve as the adsorption sites for many adsorbates (Ngah *et al*., 2011; Zou *et al*., 2011; Lin and Zhan, 2012). However, chitosan is soft and soluble in weak organic acid and other acidic media which renders it unsuitable for adsorbing in an acidic environment (Zhang and Bai, 2003; Ngah *et al*., 2008; Zhao *et al*., 2008; Ngah *et al*., 2011; Zou *et al*., 2011; Deng *et al*., 2012; Lin and Zhan, 2012). Alternatively, chemical modification (in composite form) can render the chitosan to be insoluble in acidic medium while improving its mechanical strenght and resistance to chemical degradation (Zhang and Bai, 2003; Ngah *et al*., 2008; Ngah *et al*., 2011). Different kinds of substances have been used to form composite with chitosan such as zeolite (Lin and Zhan, 2012), polyethyleneterephthalate (Zhang and Bai, 2003), epichlorohydrin (Ngah *et al*., 2008), attapulgite (Zou *et al*., 2011; Deng *et al*., 2012), fly ash (Wen *et al*., 2011), epichlorohydrin-clay (Tirtom *et al*., 2012), active carbon (Hydari *et al*., 2012), montmorillonite (Nesic *et al*., 2012), silica (Al-Sagheer and Muslim, 2010; Gandhi and Meenakshi, 2012a; 2012b; Zulfikar *et al*., 2013, and alumina (Gandhi *et al*., 2010). Silicon precursor shows quick in situ development of the silica network in the presence of ethanol and water via the sol gel route forming glassy, homogeneous and transparent films compatible over a wide composition range (Retuert *et al*., 1997), making interfacial interaction increased, greater ceramic nature, and improved thermal, mechanical, optical and adsorbing properties in form composite with chitosan (Al-Sagheer and Muslim, 2010). Although chitosan-silica composite (CSC) has been investigated as an adsorbent to remove lignosulfonate compound from aqueous solution (Zulfikar *et al*., 2013), the study on the property of CSC for humic acid removal from peat water has not been reported.

In this study, CSC were synthesized and then used to remove of humic acid from peat water. The CSC was characterized by Fourier transform infrared (FTIR) spectroscopy, scanning electron microscope (SEM), X-ray diffraction (XRD), N_2 adsorption-desorption isotherm and zeta potential. The effects of contact time, CSC dosage, pH solution and temperature on the humic acid removal were investigated. The kinetics of removal process was determined using pseudo-first-order, pseudo second-order kinetics and intra-particle-diffusion models. The Langmuir, Freundlich and Sips isotherm models were used to evaluate the equilibrium adsorption data.

MATERIALS & METHODS

Sample of chitosan (CS) prepared from shells of prawns was kindly donated from Organic Synthesis Laboratory, Department of Chemistry, Institut Teknologi Bandung, Indonesia. Acetic acid and tetraorthosilicate (TEOS) were purchased from Aldrich. Sodium hydroxide and hydrochloric acid used to adjust pH was purchased from Merck. Water used was generated from aqua demineralization system. All materials were used without further purification. Chitosan was dissolved in 1 % acetic acid solution to produce a 1 wt% chitosan solution. This solution was stirred for 24 hours at room temperature to form a homogeneous mixture. For cross linking chitosan with silica, a solution of TEOS was prepared by mixing the ethanol, water and TEOS with the ratio of TEOS:ethanol:water was 2:2:1. This solution was allowed stirring for 1.5 hours at room temperature. To this solution, the previously prepared chitosan solutions were added with the ratio of chitosan:TEOS was 1:4 and stirred for 1.5 hour at room temperature. The resulting solution was cast onto a Petri disk (with diameter of 10 cm) and dried at ambient temperature for 24 hours. After that, the resulting CSC was washed

with aqua dm until neutral and then dried under vacuum for 24 hours at 100 °C. Finally, the newly formed, dried CSC were ground using mortar and sieved to a constant size (~75 μm). The reaction between chitosan and TEOS to produce CSC could be seen at (Al-Sagheer and Muslim, 2010; Zulfikar *et al*., 2013). The peat water sample was obtained from Rimbo Panjang, a sub district of Kampar in Riau Province, Indonesia. Before mixing the peat water sample with adsorbent, its pH value was adjusted using NaOH and HCl (Merck, Germany) with 0.1 M in concentration. The pH value was measured using 300 Hanna Instrument (USA) pH meter. The characteristic of peat water sample can be seen at Table 1.

Table 1. The characteristic of peat water sample

Parameters	Unit	Result
Color	Pt-Co	492
Organic compounds	mg/L $KMnO_4$	254
pH	-	4.12
Conductivity	μS/cm	74
Turbidity	mg/L SiO_2	7.2
Iron	mg/L	0.2
Manganese	mg/L	0.1
Calcium	mg/L	0
Magnesium	mg/L	5.4

In order to identify the presence of functional groups in the CSC, Fourier transform infra red spectroscopic model 8300 IR-TF (Shimadzu, Japan) was performed in the range of 400 – 4000/cm using a KBr disc technique. The surface morphology of CSC was observed using a scanning electron microscope (JEM-2010, JEOL, Japan). To examine the crystallinity of the CSC, X-ray diffraction of sample were recorded using RINT 2000 (Rigaku Instrument Corp., Japan) with Cu Kα radiation. The surface area and average pore diameter of CSC were determined using a Micromeritics Gemini 2370 (USA) gas adsorption surface analyzer according BET multipoint technique. The zeta potential of CSC as a function of pH in 0.01 mol/L sodium chloride was measured using a Zeta Plus 4 Instrument (Brookhaven Instruments Corp., USA). For pH determination, 1 g of the dry, powdered CSC sample was mixed with 100 mL of bidistilled water and allowed to equilibrium for 3 days in a glass stoppered bottle. The batch adsorption experiments were conducted to evaluate humic acid removal from peat water over CSC at pH of 4.12 and 25°C. Typically, 5 g of the CSC were introduced into a 100 mL Teflon-line capped glass tube containing 50 mL of peat water solution (pH 4.12). The tubes were transferred into a shaker bath (Innova 3000, 3000), in which the tubes were shaken with shaking speed at 100 rpm at 25, 45, 55 and 65 °C for 2, 5, 10, 15, 20, 25, 30, 45, 60, 75, 120, 180 and 240 minutes. At the end of the predetermined time interval, the CSC particles were removed by centrifugation and the humic acid residual concentration was determined using an ultraviolet-visible spectrophotometer model UV-Vis 1601 (Shimadzu, Japan) with detecting wavelength at λ 400 nm (Zhang and Bai, 2003; Doulia *et al*., 2009; Zhang *et al*., 2012; Zulfikar *et al*., 2013). As the absorbance was pH-dependent, calibration lines were made for each required pH in the study. The percent of humic acid removal from peat water was calculated using the following equation:

$$\text{Removal}\,(\%) = \frac{Ci - Ce}{Ci} x100 \quad (1)$$

where C_i and C_e are initial and final concentration of humic acid (mg/L) in solution, respectively. The adsorption capacity of an adsorbent at equilibrium with solution volume V, was calculated using the following equation:

$$q_e\,(\text{mg/g}) = \frac{Ci - Ce}{m} x\ V \quad (2)$$

where C_i and C_e are the initial and final concentration of humic acid (mg/L) in solution, respectively. V is the volume of solution (L) and m is mass of adsorbent (g) used.

The effect of solution pH on the humic acid removal from peat water onto CSC was investigated in a pH range from 2.0 to 12.0 by adjusting the pH using 0.1 M HCl and 0.1 M NaOH solution and using 5 g of CSC for 90 minutes at 25 °C and shaking speed at 100 rpm.

The effect of CSC dosage on the humic acid removal was investigated by mixing 50 mL peat water with different dosages (1, 2, 3, 5, 7, 10, 15 and 20 g) for 90 minutes and at pH of 4.12, 25 °C and shaking speed at 100 rpm.

Humic acid removal kinetics was performed by mixing 5 g of CSC with 50 ml of peat water sample at temperature of 25 °C, 45 °C and 65 °C for 15, 30, 45, 60, 75, 90 and 120 minutes, which other conditions were held constant at pH of 4.12, particle size of 75 μm and shaking speed at 100 rpm. The experimental data were calculated to determine the adsorption kinetics by using the pseudo-first-order, pseudo-second-order and intra-particle models.

RESULTS & DISCUSSION

The FTIR spectrum of CSC showed the combination of characteristic adsorption bands between chitosan and silica groups (Fig. 1). The major bands for the CSC can be assigned as follows: 3430/

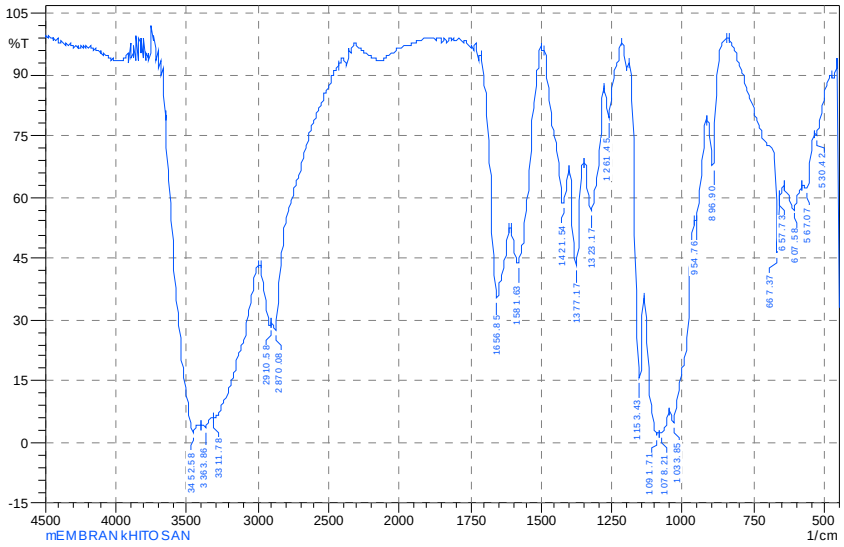

Fig. 1. FTIR spectrum of CSC adsorbent

cm (-OH stretching vibrations), 1632/cm (-NH_2 bending vibration). Other major bands observed at wave numbers of 2910/cm (-CH stretching vibration), 1377/cm (symmetric bending vibration of -CH). The adsorption band at 954 (related to the Si-OH bonds), 1078 and 801/cm (characteristics for Si-O-C absorption) indicating that there is a definite interaction between the phases (Al-Sagheer and Muslim, 2010; Zulfikar *et al*., 2013).

The surface morphologies of chitosan and CSC at 5000x magnification were shown in Fig. 2. It was observed that the surface of the chitosan prior to the cross-linking process was smooth and less porous. However, after cross-linking, the surface morphology became coarser and more porous. The silica particles are in the form of white round beads, and their dispersion within the matrix is clearly visible.

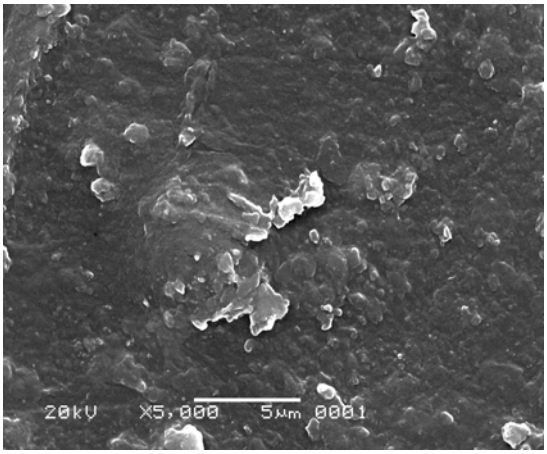

Fig. 2. Surface morphology of CSC adsorbent

From XRD pattern of silica gel, chitosan flakes and CSC (Fig. not shown here), it was found that the silica gel have characteristic peaks at 2θ = 11.6°, 20.7°, 25.6°, 29.7°, 31.7° and 49.22° and chitosan flakes have characteristic peaks at 2θ = 10.1°, 20.3°, 26.0° and 42.0°. These peaks correspond to a crystalline structure of silica gel and chitosan respectively (Gandhi and Meenakshi, 2012a; 2012b). XRD spectra of CSC are more or less amorphous in nature with small crystalline area between 2θ = 20-29°. The decrease in the crystallinity may be due to introduction of bulky chitosan polymeric chain, which demonstrates that the conjugation of silica and chitosan suppressed the crystallization to some extent. It suggests that silica and chitosan polymeric chain were mixed well at a molecular level (Gandhi and Meenakshi, 2012a; 2012b).

The surface charged characteristics of CSC was examined by measuring its zeta potential. Fig. 3 presents the zeta potential of CSC as a function of the pH solution values. The zeta potentials are positive for pH below 6.2, which this can be attributed to the protonation of amino groups in the CSC. Above pH 6.2, the zeta potential of CSC was negative. This may due to the deprotonation of amino and silanol groups in CSC. The point of zero zeta potential was obtained at about pH 6.2 which is close to the pKa value of 6.3-6.6 for amino groups in chitosan reported by other (Zhang and Bai, 2003; Zulfikar *et al*., 2013).

N_2 adsorption/desorption isotherm of CSC and its pore size distribution is illustrated in Figs 4a and 4b. As shown in Fig. 4a, CSC showed a type IV N_2 adsorption isotherm shape with an evident hysteresis loop at relative pressure range of 0.4-0.7, suggesting the presence of mesopores in CSC (Tao *et al*., 2010;

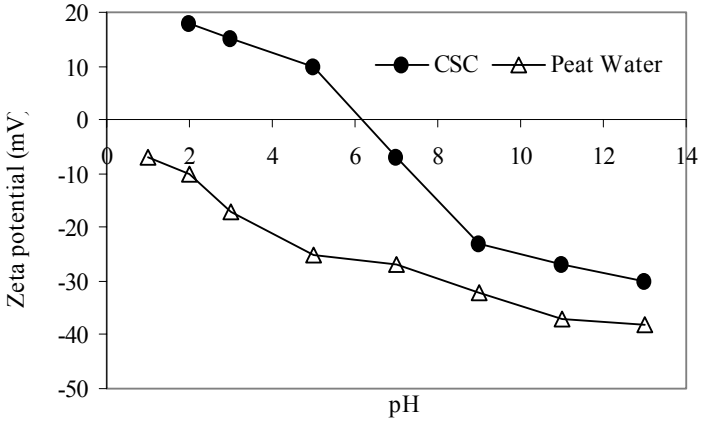

Fig. 3. Effect of pHs on the zeta potential of CSC adsorbent

Lin and Zhan, 2012). Moreover, it can see been that the hysteresis loop shift approach relative pressure (P/P_o) = 1, indicating the existence of macropores in CSC (Lin and Zhan, 2012). This conclusion agreed with the BJH pore diameter distribution of CSC (Fig. 4b), which showed that the CSC had a wide pore diameter distribution in both mesoporous and macroporous domains. The calculated BET surface area, pore volume and pore diameter are summarized in Table 2.

The effect of the contact time and temperature on the percentage of adsorption of humic acid from peat water using CSC is presented in Fig. 5. The percentage

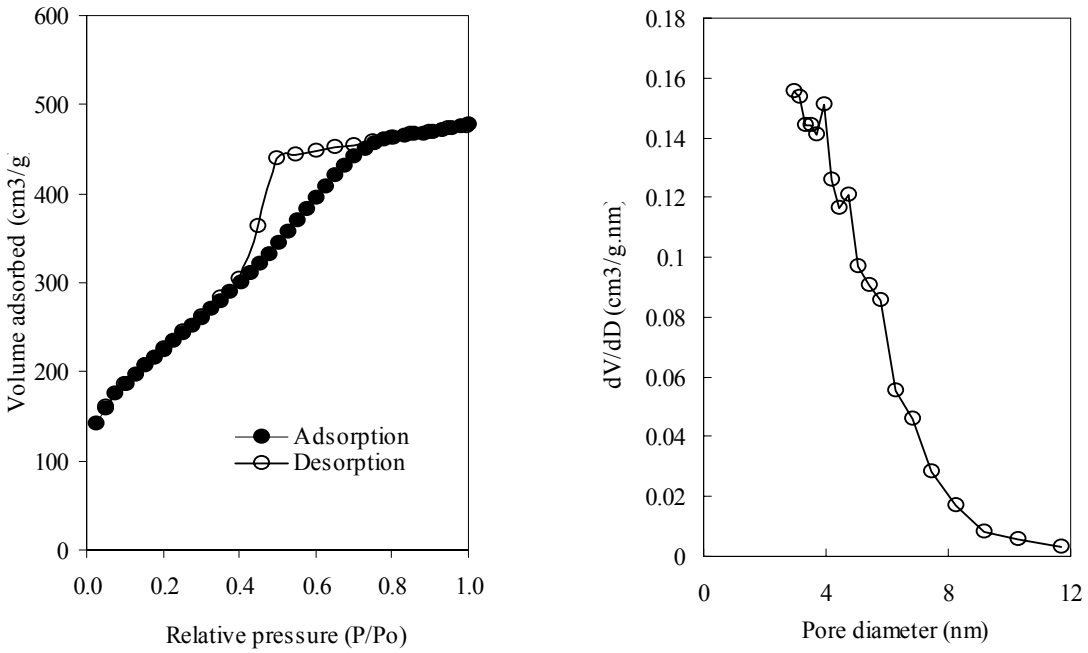

Fig. 4. (a) N_2 adsorption-desorption isotherm and (b) pore size distribution of CSC

Table 2. Characteristics of CSC adsorbent

Parameters	Values
Surface area (m^2/g)[a]	426.76
Pore diameter (nm)[b]	2.98
Total pore volume (cm^3/g)	0.50

[a] Applying BJH model
[b] Applying BJH model

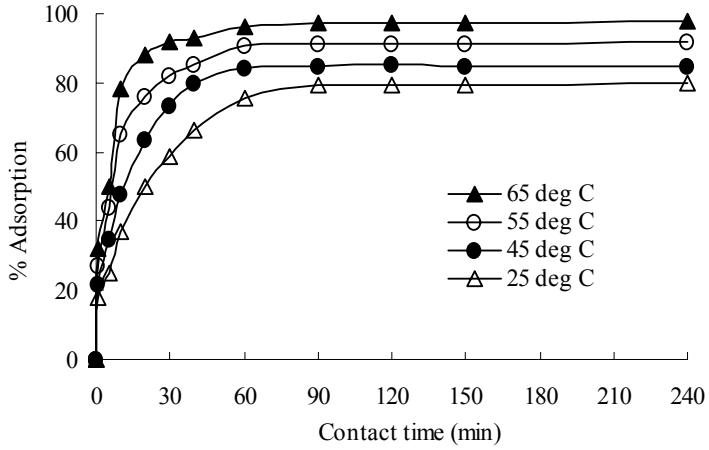

Fig. 5. Effect of contact time and temperature on humic acid removal from peat water (volume 50 mL, dosage 5 g, pH 4.12, particle size 75 μm, shaking speed 100 rpm)

of adsorption increased with increase in agitation time and reached a constant value with the increase in contact time. A rapid increased is observed for the first 25 minutes and it then proceeds slowly until reached equilibrium. This may due to the increased in the number of vacant surface sites available at initial stage. The sorption equilibrium was achieved during the same period of 90 minutes.

As shown in Fig. 5, the amount of humic acid adsorption using CSC increases with the increasing of temperature. This arises from the increase in the mobility of humic acid molecule with increasing temperature (Daifullah *et al*., 2004; Wang and Zhu, 2007; Doulia *et al*., 2009; Moussavi *et al*., 2011; Rahchamani *et al*., 2011) and more molecules across the external boundary layer and the internal pores of the adsorbent particles. Furthermore, increasing temperature may produce a swelling effect within the internal structure of adsorbent, penetrating the large humic acid molecule further (Fan *et al*., 2011; Rahchamani *et al*., 2011; Zulfikar and Setiyanto, 2013; Zulfikar *et al*., 2013b).

To optimize the adsorbent dosage for the adsorption of humic acid from peat water, adsorption investigations were carried out with different adsorbent dosages. The amounts of humic acid removed by adsorption on CSC are presented in Fig. 6. It is observed that, the percentage adsorption of the humic acid increases with increasing dosages. A significant increase in the adsorption process was observed, where the adsorption amount increased from 1 to 5 g, and any further addition of adsorbent did not cause any significant change in the percentage of adsorption. Increased humic acid adsorption with increasing CSC dosage is attributed to the increase of total adsorbent surface area and adsorption site. Almost optimum adsorption was observed in the case of 5 g of CSC. Thus, in all subsequent kinetic studies, the amount of CSC was chosen as 5 g.

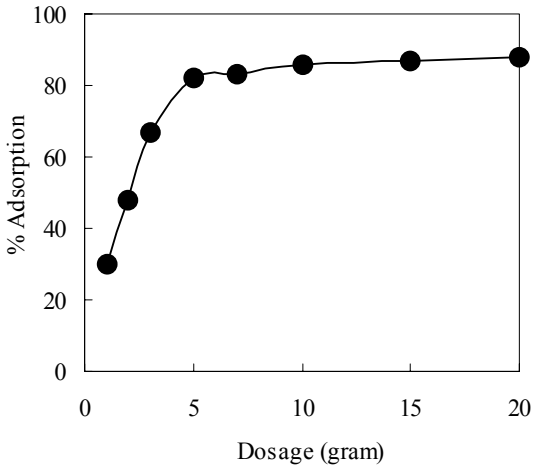

Fig. 6. Effect of adsorbent dosage on humic acid removal from peat water (contact time: 90 min., volume 50 mL, pH 4.12, particle size 75 μm, shaking speed 100 rpm, and temp. 25 °C)

The effect of initial pH of the peat water on the percentage of humic acid adsorbed was studied by varying the initial pH of peat water and keeping the other process parameters as constant. The results are shown in Fig. 7. As shown in Fig. 7, the increase in initial pH of the peat water decreased the percentage of humic acid adsorbed.

It was stated that CSC contain polar functional groups such as amino and silanol groups in their molecular structure, which can be involved in adsorption. At low pH, the concentration of H^+ ion in

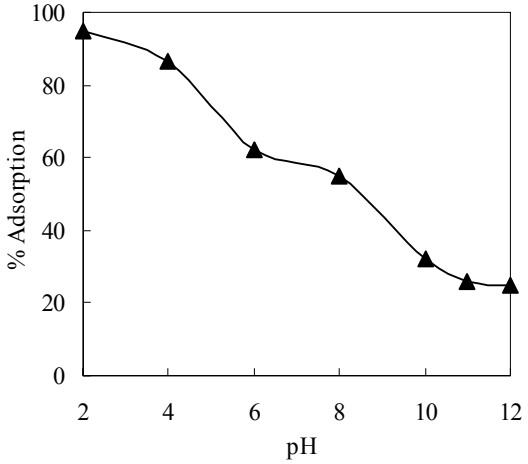

Fig. 7. Effect of pHs on humic acid removal from peat water (contact time: 90 min., volume 50 mL, dosage 5 g, particle size 75 mm, shaking speed 100 rpm, and temp. 25 °C)

the system increase and these functional groups were protonated, and the surface of the adsorbent acquiring a positive charge, as confirmed by zeta potential measurement (Fig. 3). As previously explained, humic acid is the main components of peat water, which consist of many phenolic and carboxylic functional groups. As known, the phenolic and carbonyl functional group can be ionized in aqueous medium and may acquire a negative charge in aqueous medium. On the other hand, the humic acid molecules became more negatively charged as pH value increased due to ionization of carboxylic and phenolic groups of humic acid (Fig. 3). This ionization would lead to an increase of negative charge of humic acid molecules, thus the humic acid ion will be attracted to the surface of the adsorbent by electrostatic interaction. Meanwhile at high pH, more hydroxyl ions are present in the bulk solution and the functional groups on the CSC surface were deprotonated are, so the surface charge is negative (Fig. 3). These will reduce the electrostatic attraction between the CSC surface and humic acid compound because the less positive or more negative surface charges. This decreases the adsorption rate of humic acid. To further understand the adsorption mechanism, Langmuir, Freundlich and Sips isotherm models were used to analyze the experimental results. The Langmuir isotherm model assumes that the forces of interaction between the adsorbed adsorbate molecules are negligible and once the adsorbate molecule occupies the adsorption site no further adsorption will take place. The non-linear form of Langmuir isotherm is expressed as:

$$q_e = \frac{q_m . b . C_e}{1 + b . C_e} \quad (3)$$

where C_e is the concentration of humic acid in peat water at equilibrium (mg/L), q_e is the humic acid adsorption capacity for absorbent at equilibrium (mg/g), q_m is the maximum adsorption capacity (mg/g) and K_L is Langmuir constants related to energy of adsorption (L/mg). The Freundlich adsorption isotherm model is empirical equation applicable for description of the adsorption process, which based on the assumption that the adsorbent has a heterogeneous surface composed of different adsorptive site. The Freundlich equation can be represented as:

$$q_e = K_f C_e^{1/n} \quad (4)$$

where C_e is the equilibrium concentration (mg/L), K_f (L/g) and n are Freundlich constants related to adsorption capacity of adsorbent and adsorption intensity, respectively. The value $1/n$ gives an indication of the favorability of adsorption. It has been reported that $1/n$ value between 0 and 1 represents favorable adsorption (Ghandi *et al*., 2010; Moussavi *et al*., 2011; Rachamani *et al*., 2011; Wen *et al*., 2011; Zou *et al*., 2011; Gandhi and Meenakshi, 2012a; 2012b; Lin and Zhan, 2012). Sips model is a three-parameter isotherm model that is basically a combination of Langmuir and Freundlich models, having features of both Langmuir and Freundlich equations. It is expressed as:

$$q_e = \frac{q_m . K_{eq} . C_e^{\ n}}{1 + K_{eq} . C_e^{\ n}} \quad (5)$$

where K_{eq} (L/mg) represents the equilibrium constant of the Sips equation and q_m (mg/g) is the maximum adsorption capacity. The Sips isotherm model is characterized by the heterogeneity factor, n, and specifically when n = 1, the Sips isotherm equation reduces to the Langmuir equation and it implies a homogenous adsorption process (Chatterjee *et al*., 2009; Chatterjee *et al*., 2011; Zulfikar *et al*., 2013b).

As seen from Fig. 8, Langmuir isotherm models are fitting well to the experimental data for humic acid adsorption than the Freundlich and Sips isotherm models, indicating that the adsorption of humic acid from peat water on CSC is a monolayer adsorption. In addition, the isotherm parameters from the models indicate that the Langmuir isotherm produces a better fitting result in terms of regression coefficient (Table 3). Based on the Langmuir isotherm model, the maximum adsorption of humic acid from peat water on CSC at pH 4.12 and 25 °C was found to be 120.2 mg/g.

In order to investigate the adsorption mechanism of humic acid onto CSC, the kinetic data obtained were analysis using the pseudo-first-order adsorption, the

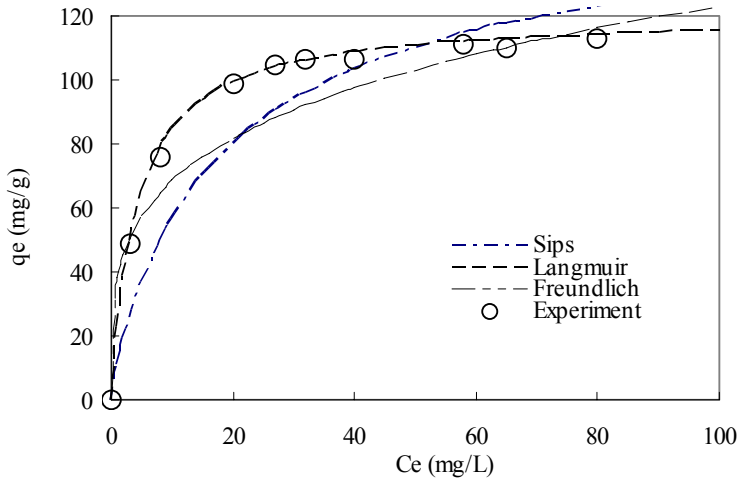

Fig. 8. Isotherm curve for humic acid removal from peat water (contact time: 90 min., volume 50 mL, pH 4.12, particle size 75 µm, dosage 5 g, shaking speed 100 rpm, and temp. 25 °C)

Table 3. Langmuir, Freundlich and Sips constants for humic acid adsorption*)

Langmuir Model			Freundlich Model			Sips Model			
b (L/mg)	q_m (mg/g)	R^2	n	K_f (mg/g)	R^2	q_m (mg/g)	K_{eq} (mL/g)	n	R^2
0.236	120.2	0.997	3.937	38.20	0.966	126.5	0.095	0.864	0.986

pseudo-second-order adsorption and the intra-particle diffusion models. The pseudo-first-order rate expression was evaluated with the following equation:

$$\log (q_e - q_t) = \log q_e - k/2.303 . t \qquad (6)$$

where q_e and q_t are the amounts of humic acid, (mg/g) adsorbed on adsorbents at equilibrium, and at time t, respectively and k is the rate constant (min^{-1}). The value of q_e, k and correlation coefficient were determined from the linear plots of log ($q_e - q_t$) against t. The adsorption rate constants and linear regression values for pseudo-first-order under different temperature were summarized in Table 4. From Table 4, we can see that the theoretical q_e values calculated from the pseudo-first-order kinetic model did not agree with the experimental values, and the correlation coefficients were also found to be slightly lower. These results indicated that the pseudo-first-order kinetic model (Fig. not shown) was not appropriate for modeling the adsorption of humic acid onto CSC.

The pseudo-second-order rate equation assumes that the adsorption capacity is proportional to the number of active sites on the surface. The pseudo-second-order equation is expressed as:

$$t/q_t = 1/k.q_e^2 + t/q_e \qquad (7)$$

where q_e and q_t are the amounts of organic compounds, (mg/g) adsorbed on sorbents at equilibrium, and at time t, respectively and k is the rate constant (g/mg.min^{-1}). k and q_e can be obtained from the intercept and slope of plotting t/q_t against t. Plot

Table 4. The pseudo-first order and second-order kinetic parameters for humic acid removal from peat water using CSC

Temperature (°C)	Pseudo-first-order			Pseudo-second-order			
	k (min^{-1})	q_e, cal (mg/g)	R^2	k (min^{-1})	q_e, cal (mg/g)	R^2	q_e, exp (mg/g)
25	0.065	2.602	0.978	0.034	3.377	0.993	3.176
45	0.077	2.793	0.990	0.057	3.539	0.998	3.400
55	0.081	2.712	0.984	0.078	3.755	0.999	3.648
65	0.147	3.305	0.994	0.105	3.970	0.999	3.888

of t/q_t against t for pseudo-second-order model under different temperature are shown in Fig. 9. From the slope and intercept values, q_2 and k_2 were calculated and the results are shown in Table 4. The linear plots of t/q_t versus t show a good agreement with experimental data giving the correlation coefficients close to 1. Also, the calculated q_2 values agree very well with the experimental data at all temperature. This means that the adsorption kinetics of humic acid onto CSC obeys the pseudo-second-order kinetic model for the entire adsorption period.

The pseudo-second-order kinetic model cannot give a definite mechanism of adsorption. Adsorption kinetics is usually controlled by different mechanisms, the most general of which is the diffusion mechanism. The intra-particle diffusion model can be defined as:

$$q_t = k.t^{0.5} + C \quad (8)$$

where k is the intra-particle diffusion rate constant (mg/g $min^{1/2}$) and q_t is the amount of humic acid adsorbed at time t (mg/g). The plot of q_t versus $t^{1/2}$ would result in a linear relationship. If the lines passed through the origin diffusion would be the controlling step. Otherwise, the intra-particle diffusion is involved in the sorption process but is not the only rate-controlling step. According to this model, the relationship between q_t against $t^{1/2}$ is shown in Fig. 10. The plot obtained for each temperature may include two stages: (a) the first part is due to boundary layer diffusion or external surface adsorption, and (b) the second stage is a gradual adsorption stage attributed to intra-particle diffusion. Extrapolating the linear portion of the plot to the ordinate produces the intercept (C) which is proportional to the extent of boundary layer thickness (Tao *et al*., 2010; Lin and Zhan, 2012; Zou *et al*., 2011; Zulfikar *et al*., 2013a; 2013b; Zulfikar and Setiyanto, 2013; Fan *et al*., 2011; Elkady *et al*., 2011; Wang *et al*., 2013).

Since the second stages of plot q_t against $t^{1/2}$ does not pass through the origin, the intra-particle diffusion is not the only rate limiting mechanism in the adsorption process (Ngah *et al*., 2008; Doulia *et al*., 2009; Hydari *et al*., 2012; Lin and Zhan, 2012; Nesic *et al*., 2012; Wang *et al*., 2013; Zulfikar *et al*., 2013a; Zulfikar and Setiyanto, 2013).

Table 5 shows the intra-particle diffusion constants (k_{d1}, k_{d2}) and the correlation coefficient (r^2). From Table 5, it can be seen that the order of the sorption rate was

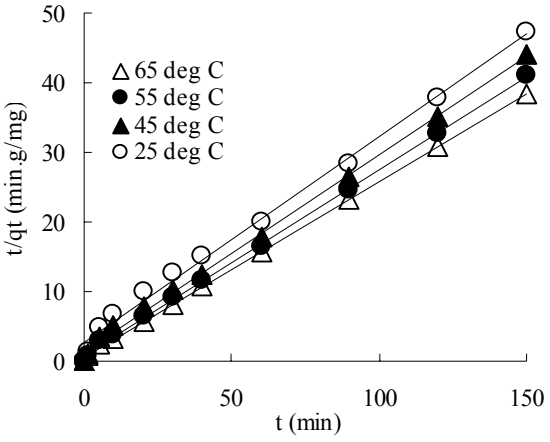

Fig. 9. Pseudo-second-order model plots for humic acid removal from peat water at different temperature (volume 50 mL, dosage 5 g, pH 4.12, particle size 75 µm, shaking speed 100 rpm)

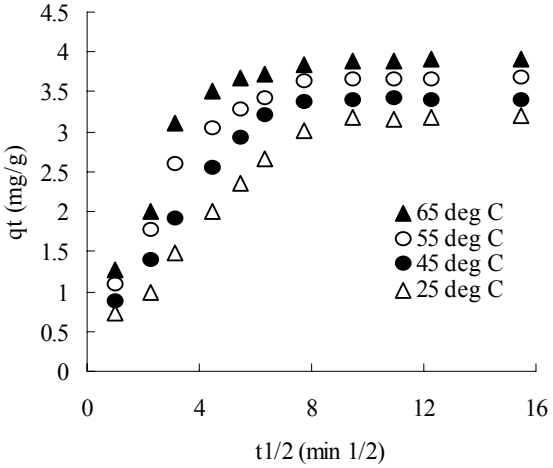

Fig.10. Intra-particle model plot for humic acid removal from peat water at different temperature (volume 50 mL, dosage 5 g, pH 4.12, particle size 75 µm, shaking speed 100 rpm)

Table 5. Parameter of the intra-particle diffusion model for the humic acid removal from peat water using CSC

Temperature (°C)	k_{d1}	C_1	R_1^2	k_{d2}	C_2	R_2^2
25	0.360	0.327	0.991	0.005	3.124	0.739
45	0.447	0.455	0.995	0.002	3.376	0.299
55	0.504	0.701	0.953	0.007	3.573	0.917
65	0.682	0.628	0.949	0.007	3.806	0.636

higher in the first stage (k_{d1}) than in the second stage (k_{d2}). That gives prediction that the humic acid removal process may be controlled by the intra-particle diffusion (Elkady *et al*., 2011; Fan *et al*., 2011; Zulfikar *et al*., 2013a; 2013b). The values of k_{d1} dan k_{d2} for the adsorption of humic acid slightly increased with increasing temperature from 25 to 65 °C. This indicated that increasing temperature slightly increases the migration of humic acid into the inner structure of CSC. From Table 5, we also can see that the value of *C* increased with increasing temperature. This suggests that the effect of boundary layer diffusion for the adsorption of humic acid on CSC probably become more important at higher temperature because of the greater random motion associated with the increased thermal energy (Lin and Zhan, 2012). The thermodynamic parameters such as the Gibbs free energy (DG^o), enthalpy (DH^o) and entropy (DS^o) were also evaluated to understand the effect of temperature on adsorption process. The thermodynamic parameters were determined using using the following equations:

$$DG^o = - RT \ln K_d \qquad (9)$$

which

$$\ln K_d = \frac{\Delta S^o}{R} - \frac{\Delta H^o}{R.T} \qquad (10)$$

where *R* (8.314 J/mol K) is the gas constant, T (K) absolute temperature and K_L (L/mg) is the Langmuir isotherm constant. The value enthalpy (DH^o) and entropy (DS^o) were calculated from the slope and intercept of the plot of ln K_L vs 1/T. The results were listed in Table 6. The positive values of Gibbs free energy (DG^o) at all temperatures showed that the removal process was non-spontaneous. The decrease of the Gibbs free energy (DG^o) change from 3.89 to 1.05 with increase temperature from 25 °C to 85 °C indicated that the presence of an energy barrier at low temperature (Wang *et al*., 2013). The value of DG^o become more negative with the increase of temperature, which indicates that the reaction is more favorable at high temperatures. The positive DH^o values obtained indicated that the sorption process was endothermic in nature. Generally, the enthalpy change (DH^o) for physical is in the range 2.1-20.9 kJ/mol and chemisorption is in the range 80-200 kJ/mol (Lin and Zhan, 2012). Since the value of DH^o observed in the system is 24.69 kJ/mol, the removal of humic acid from peat water using CSC is occurred by physisorption. The positive value of entropy change (DS^o) indicates the increased randomness at the solid-solution interface during the adsorption of humic acid onto CSC (Gandhi *et al*., 2010; Fan *et al*., 2011; Liang *et al*., 2011; Rahchamani *et al*., 2011; Lin and Zhan, 2012; Gandhi and Meenakshi, 2013a; Wang *et al*., 2013) and also reflects the greater affinity of the adsorbent for HA molecules (Liang *et al*., 2011).

The other thermodynamic parameter is activation energy (E_a). The Arrhenius equation was applied to evaluate the E_a of the adsorption process:

$$\ln k = \ln A - \frac{E_a}{R.T} \qquad (11)$$

where *k* is rate constant of pseudo-second-order kinetic model (g/mg/min), E_a is the activation energy (kJ/mol), A the Arrhenius factor, R the gas constant (8.314 J/mol K) and T is the solution absolute temperature (K). The linear plot of ln *k* versus 1/T gives a straight line with slope $-E_a$/R. The magnitude of E_a gives an opinion about the mechanism adsorption (Fan *et al*., 2011; Rahchamani *et al*., 2011; Wang *et al*., 2013). Physical adsorption typically has activation energy of 5-40 kJ/mol and chemical adsorption has activation energy of 40-800 kJ/mol (Fan *et al*., 2011; Rahchamani *et al*., 2011; Wang *et al*., 2013). The activation energy obtained in this study was 23.23 kJ/mol (Table 6) indicating that humic acid adsorption onto CSC corresponded to physisorption. The positive value of E_a suggests that an increase in temperature favors the adsorption of humic acid on SCS and the adsorption process is endothermic in nature (Lin and Zhan, 2012). A comparative evaluation of the adsorbent capacities of various types of adsorbents for the adsorption of humic acid is listed in Table 7. The adsorption capacities of the adsorbents used in this study were not among the highest available but a relatively high uptake capacity of the humic acid could be obtained which makes the adsorbents suitable for humic acid removal from peat water.

Table 6. Thermodynamic parameters for the removal of humic acid using CSC

Temperature (°C)	K_L (L/mg)	ΔG^o (kJ/mol)	ΔH^o (kJ/mol)	ΔS^o (kJ/mol)	E_a (kJ/mol)
25	0.207	3.89	24.69	69.62	23.23
45	0.361	2.69			
55	0.498	1.90			
65	0.689	1.05			

Table 7. Comparison of adsorption capacity of various adsorbent for humic acid removal

Materials	Adsorbate	q_m (mg/g)	Concentration range (mg/L)	pH	Contact time	References
Natural zeolite (20 ^oC)	Humic acid	7.7	2-20	7	-	Moussavi *et al*., 2011
Greek bentonite (35 ^oC)	Humic acid	10.75	10-200	-	5 h	Doulia *et al.*, 2009
Granular activated carbon	Humic acid	55.8	10-100	4	-	Maghsoodloo *et al.*, 2011
Unburned carbon	Humic acid	72	10-100	7	200 h	Wang and Zhu, 2007
Shorea dasyphylla sawdust	Humic acid	68.4	10-80	2	30 min	Kamari *et al*., 2009
Bentonite	Humic acid	53.0	10-150	3	24 h	Zhang *et al*., 2012
Chitosan-PET	Humic acid	0.407	10-60	6.5	60 h	Zhang and Bai, 2003
Rice husk activated carbon	Humic acid	45.4	20-150	10	-	Daifullah *et al*., 2004
Chitosan-ECH beads	Humic acid	44.8	10-50	6	1 h	Ngah *et al.*, 2008
Fly ash	Humic acid	36.0	10-100	5	170 h	Wang *et al.*, 2008
Fly ash	Humic acid	10.7	10-100	7	200 h	Wang and Zhu, 2007
Chitosan	Humic acid	28.9	0-80	3.07	25 min	Ngah and Musa, 1998
Chitin	Humic acid	27.3	0-80	2.40	25 min	Ngah and Musa, 1998
Eggshell	Peat water	126.58	-	4.01	60 min	Zulfikar *et al.*, 2013a
Am-PAA-B (30 ^oC)	Humic acid	174.03	25-100	-	4 h	Anirudhan *et al.*, 2008
Chitosan-H_2SO_4 beads (at 300 K)	Humic acid	377.4	0-70	-	60 min	Ngah *et al.*, 2011
Pillared bentonite	Humic acid	537.0	0-1300	4	24 h	Peng *et. al*., 2005
Activated carbon	Humic acid	52.4	0-200	7	24 h	Tao *et al.*, 2010
SBA-15	Humic acid	8.5	0-200	7	24 h	Tao *et al.*, 2010
APTS-SBA-15-5%	Humic acid	72.5	0-200	7	24 h	Tao *et al.*, 2010
APTS-SBA-15-10%	Humic acid	117.6	0-200	7	24 h	Tao *et al.*, 2010
ATP-PANI (at 25 ^oC)	Humic acid	52.91	5-60	5	24 h	Wang *et al.*, 2011
Chitosan-silica	Peat water	120.2	-	4.12	90 min	This study
SMCSZ	Humic acid	164	0-60	7	24 h	Lin and Zhan, 2012

CONCLUSION

These experimental studies have indicated that chitosan silica composite (CSC) has the potential to act as an adsorbent for the removal of humic acid from peat water. The results from this work showed that the adsorption of humic acid was found to increase with increase in contact time and temperature while acidic pH was more favourable for the adsorption of humic acid from peat water. The optimum dosage of CSC was 10 g. Equilibrium data were fitt ed to non-linear models of Langmuir, Freundlich and Sips, and the equilibrium data were best described by the Langmuir isotherm model, with maximum monolayer adsorption capacity of 120.2 mg/g at 25 ^{o}C and pH 4.12. Kinetic data were tested using the pseudo-first-order, pseudo-second-order kinetic models and intra-particle equations. The kinetics of the adsorption process was found to follow the pseudo-second-order kinetic model, with a rate constant in the range of 0.034 - 0.105 g/mg/min. Intra-particle diffusion model was applied to identify the adsorption mechanism and this model indicated that intra-particle diffusion was the main rate determining step in humic acid removal process. The value of adsorption energy, E_a, gives an idea about the nature of sorption. From the value of the activation energy of the process, it was concluded that the adsorption of humic acid by CSC is physical sorption. The adsorption dependence of humic acid on temperature was investigated and the thermodynamic parameters were calculated. Thermodynamic parameters data indicated that the humic acid sorption process was non-spontaneous and endothermic under the experimental conditions, with the Gibbs free energy (ΔG^o) in the range of 1.05-3.89 kJ/mol, enthalpy (ΔH^o) and entropy (ΔS^o) of 24.69 kJ/mol and 69.62 J/mol, respectively and the activation energy was 23.23 kJ/mol. The results revealed that the process of humic acid adsorption is favoured at high temperatures.

ACKNOWLWDGEMENT

The authors are very grateful to authorities of the Organic Synthesis Laboratory, Department of Chemistry, Institut Teknologi Bandung, Indonesia for kindly providing the chitosan-silica samples for this research study.

REFERENCES

Abate, G. and Masini, J. C. (2003). Influence of pH and ionic strength on removal processes of a sedimentary humic acid in a suspension of vermiculite. Colloids Surf. A, **226**, 25-34.

Albers, C. N., Banta, G. T., Hansen, P. E. and Jacobsen, O. S. (2008). Effect of different of humic substances on the fate of diuron and its main metabolite 3,4-dichloroaniline in soil. Environ. Sci. Technol., **42**, 8687-8691.

Al-Sagheer, F. and Muslim, S. (2010). Thermal and mechanical properties of chitosan/SiO_2 hybrid composites. J. Nanomater., DOI: 10.1155/2010/490679.

Anirudhan, T. S., Suchithra, P. S. and Rijith, S. (2008). Amine-modified polyacrylamide-bentonite composite for the adsorption of humic acid in aqueous solution. Colloids Surf. A, **326**, 147-156.

Chatterjee, S., Lee, D. S., Lee, M. W. and Woo, S. H. (2009). Enhance adsorption of congo red from aqueous solutions by chitosan hydrogel beads impregnated with cetyl trimethyl ammonium bromide. Bioresource Technol., **100**, 2803-2809.

Chatterjee, S., Chatterjee, T. and Woo, S. H. (2011). Adsorption of Congo Red from aqueous solution using chitosan hydrogel beads formed by various anionic surfactants. Sep. Sci. Technol., **46**, 986-996.

Daifullah, A. A. M., Girgis, B. S. and Gad, H. M. H. (2004). A study of the factors affecting the removal of humic acid by activated carbon prepared from biomass material. Colloids Surf. A, **235**, 1-10.

Deng, Y. H., Wang, L., Hu, X. B., Liu, B. Z., Wei, Z. B., Yang, S. G. and Sun, C. (2012). Highly efficient removal of tannic acid from aqueous solution by chitosan-coated attapulgite. Chem. Eng. J., **181-182**, 300-306.

Doulia, D., Leodopoulos, C., Gimouhopoulos, K. and Rigas, F., (2009). Adsorption of humic acid on acid-activated Greek bentonite. J. Colloid Interface Sci., **340**, 131-141.

Elkady, M. F., Ibrahim, A. M. and Abd El-Latif, M. M. (2011). Assessment of the adsorption kinetics, equilibrium and thermodynamic for the potential removal of reactive red dye using eggshell biocomposite beads. Desalination, **278**, 412-423.

Fan, J., Cai, W. and Yu, J. (2011). Adsorption of N719 dye on anatase TiO_2 nanoparticles and nanosheets with exposed (001) facets: Equilibrium, kinetic, and thermodynamic studies. Chem. Asian J., **6**, 2481-2490.

Gandhi, M.R., Viswanathanb, N. and Meenakshia, S. (2010). Preparation and application of alumina/chitosan biocomposite. Int. J. Biology Macromol., **47**, 146-154.

Gandhi, M. R. and Meenakshi, S. (2012a). Preparation and characterization of La(III) encapsulated silica gel/chitosan composite and its metal uptake studies. J. Hazard. Mater., **203-204**, 29-37.

Gandhi, M. R. and Meenakshi, S. (2012). Preparation and characterization of silica gel/chitosan composite for the removal of Cu(II) and Pb(II). Int. J. Biology Macromol., **50**, 650-657.

Garci´a, M. A. F., Utrilla, J. R., Toledo, I. B. and Castilla, C. M. (1998). Adsorption of humic substances on activated carbon from aqueous solutions and their effect on the removal of Cr (III) ions. Langmuir, **14**, 1880-1886.

Ghernaout, D., Ghernaout, B., Saibaa, A., Boucherita, A. and Kellil, A. (2009). Removal of humic acids by continuous electromagnetic treatment followed by electrocoagulation in batch using aluminium electrodes. Desalination, **239**, 295-308.

Gupta, V. K., Carrott, P. J. M., Carrott, M. M. L. R. and Suhas. (2009). Low-cost adsorbents: Growing approach to wastewater treatment – a review. Critical Review Environ. Sci. Technol., **39**, 783-842.

Hamid, N. A. A., Ismail, A. F., Matsuura, T., Zularisam, A. W., Lau, W. J., Yuliwati, E. and Abdullah, M. S. (2011). Morphological and separation performance study of polysulfone/titanium dioxide (PSF/TiO_2) ultrafiltration membranes for humic acid removal. Desalination, **273**, 85-92.

Hydari, S., Sharififard, H., Nabavinia, M. and Parvizi, M. R. (2012). A comparative investigation on removal performances of commercial activated carbon, chitosan biosorbent and chitosan/activated carbon composite for cadmium. Chem. Eng. J., **193-194**, 276-282.

Kamari, A., Ngah, W. S. W. and Wong, L. W. (2009). *Shorea dasyphylla* sawdust for humic acid adsorption. Eur. J. Wood Prod., **67**, 417-426.

Katsoufidou, K. S., Sioutopoulos, D. C., Yiantsios, S. G. and Karabelas, A. J. (2010). UF membrane fouling by mixtures of humic acids and sodium alginate: Fouling mechanisms and reversibility. Desalination, **264**, 220-227.

Liang, L., Luo, L. and Zhang, S. (2011). Adsorption and desorption of humic and fulvic acids on SiO_2 particles at nano- and micro-scales. Colloids Surf. A, **384**, 126-130.

Libecki, B. and Dziejowski, J. (2008). Optimization of humic acids coagulation with aluminum and iron (III) salts. Polish J. Environ. Studies, **17 (3)**, 397-403.

Lin, J. and Zhan, Y. (2012). Adsorption of humic acid from aqueous solution onto unmodified and surfactant-modified chitosan/zeolite composites. Chem. Eng. J., **200-202**, 202-213.

Maghsoodloo, S., Noroozi, B., Haghi, A. K. and Sorial, G. A. (2011). Consequence of chitosan treating on the adsorption of humic acid by granular activated carbon. J. Hazard. Mater., **191**, 380-387.

Moussavi, G., Talebi, S., Farrokhi, M. and Sabouti, R. M. (2011). The investigation of mechanism, kinetic and isotherm of ammonia and humic acid co-adsorption onto natural zeolite. Chem. Eng. J., **171**, 1159-1169.

Nesic, A. R., Velickovic, S. J. and Antonovic, D. G. (2012). Characterization of chitosan/montmorillonite membranes as adsorbents for Bezactive Orange V-3R dye. J. Hazard. Mater., **209-210**, 256-263.

Ngah, W. S. W. and Musa, A. (1998). Adsorption of humic acid onto chitin and chitosan. J. App. Polym. Sci., **69**, 2305-2310.

Ngah, W. S. W., Hanafiah, M. A. K. M. and Yong, S. S. (2008). Adsorption of humic acid from aqueous solutions on crosslinked chitosan-epichlorohydrin beads: Kinetics and isotherm studies. Colloids Surf. B, **65**, 18-24.

Ngah, W. S. W., Fatinathan, S. and Yosop, N. A. (2011). Isotherm and kinetic studies on the adsorption of humic acid onto chitosan-H_2SO_4 beads. Desalination, **272**, 293-300.

Park, S. and Yoon, T. (2009). Effects of iron species and inert minerals on coagulation and direct filtration for humic acid removal. Desalination, **239**, 146-158.

Peng, X., Luan, Z., Chen, F., Tian, B. and Jia, Z. (2005). Adsorption of humic acid onto pillared bentonite. Desalination, **174**, 135-143.

Rahchamani, J., Moausavi, H.Z. and Behzad, M. (2011). Adsorption of methyl violet from aqueous solution by polyacrylamide as an adsorbent: Isotherm and kinetic studies. Desalination, **267**, 256-260.

Retuert, J., Nunez, A., Martinez, F. and Yazdani-Pedram, M. (1997). Synthesis of polymeric organic-inorganic hybrid materials. Partially deacetylated chitin-silica hybrid. Macromol. Rapid Com., **18 (2)**, 163-167.

Rojas, J. C., Pérez, J., Garralón, G., Plaza, F., Moreno, B. and Gómez, M. A. (2011). Humic acids removal by aerated spiral-wound ultrafiltration membrane combined with coagulation–hydraulic flocculation. Desalination, **266**, 128-133.

Salman, M., El-Eswad, B. and Khalili, F. (2008). Adsorption of humic acid on bentonite. App. Clay Sci., **38**, 51-56.

Sonea, D., Pode, R., Manea, F., Ratiu, C., Lazau, C., Grozescu, I. and Burtica, G. (2010). The comparative assessment of photolysis, sorption and photocatalysis processes to humic acids removal from water. Chemical Bulletin of "POLITEHNICA" Univ. (Timisoara) 55 (69) 148-151.

Sun, C., Yue, Q., Gao, B., Mu, R., Liu, J., Zhao, Y., Yang, Z. and Xu, W. (2011). Effect of pH and shear force on flocs characteristics for humic acid removal using polyferric aluminum chloride organic polymer dual-coagulants. Desalination, **281**, 243-247.

Tao, Q., Xu, Z., Wang, J., Liu, F., Wan, H. and Zheng, S. (2010). Adsorption of humic acid to aminopropyl functionalized SBA-15. Microporous Mesoporous Mater., **131**, 177-185.

Tirtom, V.N., Dincer, A., Becerik, S., Aydemir, T. and Celik, A. (2012). Comparative adsorption of Ni(II) and Cd(II) ions on epichlorohydrin crosslinked chitosan-clay composite beads in aqueous solution. Chem. Eng. J., **197**, 379-386.

Uygunera, C.S., Suphandaga, S.A., Kercb, A. and Bekbolet, M. (2007). Evaluation of adsorption and coagulation characteristics of humic acids preceded by alternative advanced oxidation techniques. Desalination, **210**, 183-193.

Wang, S. and Zhu, Z.H. (2007). Humic acid adsorption on fly ash and its derived unburned carbon. J. Colloid Interface Sci., **315**, 41-46.

Wang, S., Terdkiatburana, T. and Tade, M. O. (2008). Single and co-adsorption of heavy metals and humic acid on fly ash. Sep. Purif. Technol., **58**, 353-358.

Wang, S., Ma, Q. and Zhu, Z.H. (2009). Characteristics of unburned carbons and their application for humic acid removal from water. Fuel Proc. Technol., **90**, 375-380.

Wang, J., Han, X., Ma, Y., Ji, Y. and Bi, L. (2011). Adsorptive removal of humic acid from aqueous solution on polyaniline/ attapulgite beads. Chem. Eng. J., **173**, 171-177.

Wang, W., Li, H., Ding, Z. and Wang, X. (2011). Effects of advanced oxidation pretreatment on residual aluminium control in high humic acid water purification. J. Environ. Sci., **23 (7)**, 1079-1085.

Wen, Y., Tang, Z., Chen, Y. and Gu, Y. (2011). Adsorption of Cr(VI) from aqueous solutions using chitosan-coated fly ash composite as biosorbent. Chem. Eng. J., **175**, 110-116.

Wang, W., Zheng, B., Deng, Z., Feng, Z. and Fu, L. (2013). Kinetics and equilibriums for adsorption of poly(vinyl alcohol) from aqueous solution onto natural bentonite. Chem. Eng. J., **214**, 343-354.

Zhao, L., Luo, F., Wasikiewicz, J.M., Mitomo, H., Nagasawa, N., Yagi, T., Tamada, M. and Yoshii, F. (2008). Adsorption of humic acid from aqueous solution onto irradiation crosslinked carboxymethylchitosan. Bioresources Technol., **99**, 1911-1917.

Zhang, X. and Bai, R. (2003). Mechanism and kinetics of humic acid adsorption onto chitosan-coated granules. J. Colloid Interface Sci., **264**, 30-38.

Zhang, L., Luo, L. and Zhang, S. (2012). Integrated investigations on the adsorption mechanisms of fulvic and humic acids on three clay minerals. Colloid Surf. A, **406**, 84-90.

Zou, X. H., Pan, J. M., Ou, H. X., Wang, X., Guan, W., Li, C. X., Yan, Y. S. and Duan, Y. Q. (2011). Adsorptive removal of Cr(III) and Fe(III) from aqueous solution by chitosan/ attapulgite composites: Equilibrium, thermodynamics and kinetics. Chem. Eng. J., **167**, 112-121.

Zulfikar, M. A., Novita, E., Hertadi, R. and Djajanti, S. D. (2013a). Removal of humic acid from peat water using untreated powdered eggshell as a low cost adsorbent. Int. J. Environ. Sci. Technol., DOI. 10.1007/s13762-013-0204-5.

Zulfikar, M. A., Wahyuningrum, D. and Lestari, S. (2013b). Adsorption of lignosulfonate compound from aqueous solution onto chitosan-silica beads. Sep. Sci. Technol., **48**, 1391-1401.

Zulfikar, M. A. and Setiyanto, H. (2013). Study of the adsorption kinetics and thermodynamic for the removal of Congo red from aqueous solution using powdered eggshell. Int. J. Chem. Tech. Res., **5(4)**, 1671-1678.